ISSN 1948-5204 (online)

World Journal of *Gastrointestinal Oncology*

World J Gastrointest Oncol 2024 July 15; 16(7): 2867-3367

Published by Baishideng Publishing Group Inc

World Journal of Gastrointestinal Oncology

Contents

Monthly Volume 16 Number 7 July 15, 2024

EDITORIAL

REVIEW

MINIREVIEWS

ORIGINAL ARTICLE

Case Control Study

Retrospective Study

World Journal of Gastrointestinal Oncology

Monthly Volume 16 Number 7 July 15, 2024

Contents

World Journal of Gastrointestinal Oncology

Monthly Volume 16 Number 7 July 15, 2024

Contents

World Journal of Gastrointestinal Oncology

Monthly Volume 16 Number 7 July 15, 2024

Contents

ABOUT COVER

Editorial Board Member of *World Journal of Gastrointestinal Oncology*, Meysam Ebrahimifar, MSc, PhD, Research Assistant Professor, Department of Toxicology, Islamic Azad University, Isfahan 1477893855, Iran. ebrahimifar67@gmail.com

AIMS AND SCOPE

The primary aim of *World Journal of Gastrointestinal Oncology* (*WJGO*, *World J Gastrointest Oncol*) is to provide scholars and readers from various fields of gastrointestinal oncology with a platform to publish high-quality basic and clinical research articles and communicate their research findings online.

WJGO mainly publishes articles reporting research results and findings obtained in the field of gastrointestinal oncology and covering a wide range of topics including liver cell adenoma, gastric neoplasms, appendiceal neoplasms, biliary tract neoplasms, hepatocellular carcinoma, pancreatic carcinoma, cecal neoplasms, colonic neoplasms, colorectal neoplasms, duodenal neoplasms, esophageal neoplasms, gallbladder neoplasms, *etc*.

INDEXING/ABSTRACTING

The *WJGO* is now abstracted and indexed in PubMed, PubMed Central, Science Citation Index Expanded (SCIE, also known as SciSearch®), Journal Citation Reports/Science Edition, Scopus, Reference Citation Analysis, China Science and Technology Journal Database, and Superstar Journals Database. The 2024 edition of Journal Citation Reports® cites the 2023 journal impact factor (JIF) for *WJGO* as 2.5; JIF without journal self cites: 2.5; 5-year JIF: 2.8; JIF Rank: 71/143 in gastroenterology and hepatology; JIF Quartile: Q2; and 5-year JIF Quartile: Q2. The *WJGO*'s CiteScore for 2023 is 4.2 and Scopus CiteScore rank 2023: Gastroenterology is 80/167; Oncology is 196/404.

RESPONSIBLE EDITORS FOR THIS ISSUE

NAME OF JOURNAL
World Journal of Gastrointestinal Oncology

ISSN
ISSN 1948-5204 (online)

LAUNCH DATE
February 15, 2009

FREQUENCY
Monthly

EDITORS-IN-CHIEF
Monjur Ahmed, Florin Burada

EDITORIAL BOARD MEMBERS
https://www.wjgnet.com/1948-5204/editorialboard.htm

PUBLICATION DATE
July 15, 2024

INSTRUCTIONS TO AUTHORS
https://www.wjgnet.com/bpg/gerinfo/204

GUIDELINES FOR ETHICS DOCUMENTS
https://www.wjgnet.com/bpg/GerInfo/287

GUIDELINES FOR NON-NATIVE SPEAKERS OF ENGLISH
https://www.wjgnet.com/bpg/gerinfo/240

PUBLICATION ETHICS
https://www.wjgnet.com/bpg/GerInfo/288

PUBLICATION MISCONDUCT
https://www.wjgnet.com/bpg/gerinfo/208

ARTICLE PROCESSING CHARGE
https://www.wjgnet.com/bpg/gerinfo/242

STEPS FOR SUBMITTING MANUSCRIPTS
https://www.wjgnet.com/bpg/GerInfo/239

ONLINE SUBMISSION
https://www.f6publishing.com

World Journal of Gastrointestinal Oncology

Submit a Manuscript: https://www.f6publishing.com

World J Gastrointest Oncol 2024 July 15; 16(7): 3193-3210

DOI: 10.4251/wjgo.v16.i7.3193

ISSN 1948-5204 (online)

ORIGINAL ARTICLE

Basic Study

Baitouweng decoction suppresses growth of esophageal carcinoma cells through miR-495-3p/BUB1/STAT3 axis

Hui Yang, Xiao-Wei Chen, Xue-Jie Song, Hai-Yang Du, Fu-Chun Si

Specialty type: Oncology

Provenance and peer review: Unsolicited article; Externally peer reviewed.

Peer-review model: Single blind

Peer-review report's classification

Scientific Quality: Grade B
Novelty: Grade B
Creativity or Innovation: Grade B
Scientific Significance: Grade B

P-Reviewer: Zaman UM, Pakistan

Received: January 20, 2024
Revised: April 29, 2024
Accepted: June 4, 2024
Published online: July 15, 2024
Processing time: 174 Days and 4.8 Hours

Hui Yang, Xiao-Wei Chen, Xue-Jie Song, Hai-Yang Du, Fu-Chun Si, Henan Key Laboratory of Traditional Chinese Medicine Syndrome and Prescription in Signaling, Henan International Joint Laboratory of TCM Syndrome and Prescription in Signaling, Traditional Chinese Medicine School, Henan University of Chinese Medicine, Zhengzhou 450046, Henan Province, China

Corresponding author: Fu-Chun Si, PhD, Professor, Henan Key Laboratory of Traditional Chinese Medicine Syndrome and Prescription in Signaling, Henan International Joint Laboratory of TCM Syndrome and Prescription in Signaling, Traditional Chinese Medicine School, Henan University of Chinese Medicine, No. 156 Jinshui East Road, Zhengdong New District, Zhengzhou 450046, Henan Province, China. sifc2000@hotmail.com

Abstract

BACKGROUND

Esophageal carcinoma (EC) is one of the most prevalent cancers in human populations worldwide. Baitouweng decoction is one of the most important Chinese medicine formulas, with the potential to treat cancer.

AIM

To investigate the role and mechanism of Baitouweng decoction on EC cells.

METHODS

Differentially expressed genes (DEGs) in EC tissues and normal tissues were screened by the cDNA microarray technique and by bioinformatics methods. The target genes of microRNAs were predicted based on the TargetScan database and verified by dual luciferase gene reporter assay. We used Baitouweng decoction to intervene EC cells, and detected the activity of EC9706 and KYSE150 cells by the MTT method. Cell cycle and apoptosis were measured by flow cytometry. The expression of *BUB1* mRNA and miR-495-3p was measured by qRT-PCR. The protein levels of BUB1, STAT3, p-STAT3, CCNB1, CDK1, Bax, Caspase3, and Caspase9 were measured by Western blot analysis. The migration and invasion abilities of the cells were measured by wound-healing assay and Transwell invasion assay, respectively.

RESULTS

DEGs identified are involved in biological processes, signaling pathways, and network construction, which are mainly related to mitosis. *BUB1* was the key hub gene, and it is also a target gene of miR-495-3p. Baitouweng decoction could

upregulate miR-495-3p and inhibit *BUB1* expression. *In vitro* experiments showed that Baitouweng decoction significantly inhibited the migration and invasion of EC cells and induced apoptosis and G2/M phase arrest. After treatment with Baitouweng decoction, the expression of Bax, Caspase 3, and Caspase 9 in EC cells increased significantly, while the expression of BUB1, CCNB1, and CDK1 decreased significantly. Moreover, the STAT3 signaling pathway may play an important role in this process.

CONCLUSION

Baitouweng decoction has a significant inhibitory effect on EC cell growth. BUB1 is a potential therapeutic target for EC. Further analysis showed that Baitouweng decoction may inhibit the growth of EC cells by upregulating miR-495-3p targeting the BUB1-mediated STAT3 signal pathway.

Key Words: Baitouweng decoction; Esophageal cancer; miR-495-3p; BUB1; STAT3 signaling pathway

Core Tip: Differentially expressed genes in esophageal carcinoma (EC) were analyzed and BUB1 was found to be a key hub gene. BUB1 is a target gene of miR-495-3p, and BUB1 can directly interact with STAT3 to inhibit tumor cell proliferation. We studied the effects of Baitouweng decoction on the cell cycle, apoptosis, migration, and invasion, and further investigated the inhibitory effect of Baitouweng decoction on the development of EC by targeting BUB1 and STAT3 *via* miR-495-3p. The potential functional pathways were explored.

Citation: Yang H, Chen XW, Song XJ, Du HY, Si FC. Baitouweng decoction suppresses growth of esophageal carcinoma cells through miR-495-3p/BUB1/STAT3 axis. *World J Gastrointest Oncol* 2024; 16(7): 3193-3210
URL: https://www.wjgnet.com/1948-5204/full/v16/i7/3193.htm
DOI: https://dx.doi.org/10.4251/wjgo.v16.i7.3193

INTRODUCTION

Esophageal carcinoma (EC) is one of the most common malignant tumors of the digestive tract with a high incidence, high degree of malignancy, and poor prognosis[1]. Currently, EC treatments include surgery, radiotherapy, chemotherapy, targeted therapy, and the combined application of various methods[2-6]. However, owing to the emergence of drug resistance, patient tolerance, and side effects during treatment, the total 5-year survival rate is less than 20%[7]. Therefore, novel therapeutic strategies are urgently required. Traditional Chinese medicine (TCM) has been used for thousands of years. Many TCM monomers and compounds have proven to be effective in the treatment of EC[8,9]. TCM has the advantages of multi-orientation, multiple targets, and multiple effects, increasing the curative effect of radiotherapy and chemotherapy, reducing side effects, improving the quality of life of patients, and not easily producing drug resistance[10-12]. The effects of TCM on EC have received increasing attention worldwide. However, there is still much room for the development of TCM to improve the understanding and treatment of EC. It is necessary to conduct in-depth research combined with literature review, data mining, epidemiological investigations, and modern clinical trial design methods to provide a basis for the popularization and application of TCM in the treatment of EC.

Baitouweng decoction was originally recorded in the classic Chinese medicine book "Treatise on Febrile Diseases" (Chinese name: Shang-Han Lun). This formula consists of four Chinese herbal medicines: *Pulsatillae Radix*, *Fraxini Cortex*, *Phellodendri Chinensis Cortex*, and *Coptidis Rhizoma*. It has the effects of clearing heat, detoxifying, cooling blood, and stopping dysentery[13]. Baitouweng decoction has good pharmacological properties, including anti-inflammatory, antibacterial, antitumor, and immune regulatory effects[14-16]. Baitouweng decoction is an important prescription for the treatment of gastrointestinal diseases[17,18]. We found that Baitouweng decoction inhibits the proliferation of EC cells[19,20]. However, there is a lack of research on the mechanism of action of this prescription for EC. Thus, we aimed to investigate the potential mechanism of Baitouweng decoction in the treatment of EC and to provide more effective strategies and ideas for screening new therapeutic targets for EC. Budding uninhibited by benzimidazole 1 (BUB1) is a mitotic checkpoint serine/threonine kinase, playing an important role in maintaining the correct segregation of chromosomes and reducing aneuploidy in mitosis[21]. BUB1 has been reported to be highly expressed in a variety of human cancers, including breast, pancreatic, gastric, and liver cancers[22-25]. BUB1 enhances NFATC2- and LHX1-induced proliferation of bladder cancer cells mediated by signal transducer and activator of transcription 3 (STAT3)[26]. However, the detailed function and regulation of BUB1 in EC require further investigation.

MicroRNAs (miRNAs) are endogenous non-coding RNAs with regulatory functions[27]. Mutations in or abnormal expression of miRNAs may be closely related to the occurrence and development of cancer[28,29]. miR-495-3p is located at human 14q32.31 site and participates in the proliferation, migration, and invasion of cancer cells[30,31]. miR-495-3p overexpression can reduce the migratory ability of EC cells and is regulated by the long noncoding RNA FAM83A-AS1 [32].

In this study, differentially expressed genes (DEGs) in EC were analyzed, and BUB1 was found to be a key hub gene. BUB1 is a target gene of miR-495-3p and directly interacts with STAT3 to inhibit tumor cell proliferation. We investigated the effects of Baitouweng decoction on the cell cycle, apoptosis, migration, and invasion, and further investigated its inhibitory effect on EC development by targeting BUB1 and STAT3 *via* miR-495-3p. Potential functional pathways were explored, with an aim to provide novel insights into the mechanism of action of Baitouweng decoction in the treatment of EC.

MATERIALS AND METHODS

Experimental materials

A total of 21 cases of EC tumor tissue and adjacent normal tissue (2 cm away from the cancer tissue) were collected from the Department of Thoracic Surgery of the First Affiliated Hospital of Henan University of Chinese Medicine. There were 16 men and 5 women with an average age of 66.23 years. All patients were pathologically diagnosed with highly or moderately differentiated EC without preoperative radiotherapy or chemotherapy. Fresh tissues were collected immediately after surgical resection, rinsed with cold PBS, and quickly stored in liquid nitrogen. This study was approved by the Medical Ethics Committee of the First Affiliated Hospital of Henan University of Chinese Medicine, and an informed consent form was signed by the patients and their families.

Gene chip technology-based genomic analysis

Genomic analyses were performed as our previous description[33]. Briefly, total RNA was extracted from EC tissues, and RNA integrity was detected using NanoDrop 2000 (Thermo Scientific, United States) and Agilent Bioanalyzer 2100 (Agilent Technologies, United States). Double-stranded cDNA was obtained by reverse transcription of total RNA and labeled with a cyanine-3-CTP (Cy3) fluorescent dye to obtain cRNA. After purification using the QIAGEN RNeasy® Mini Kit (Qiagen, Germany), the labeled cRNA was placed in a warm water bath at 60 °C for 30 min, followed by an ice water bath for 1 min. The chip was hybridized with cRNA in a hybrid furnace at 65 °C at 10 r/min for 17 h. After hybridization, the chips were eluted. The chip was then scanned using an Agilent Scanner G2505C (Agilent Technologies) and the original signal value of the chip was extracted to standardize the data and filter the probe. The original image was processed using the Feature Extraction software (version 10.7.1.1, Agilent Technologies), and the original data were obtained. GenePring software (version 12.5; Agilent Technologies) was used to standardize the original chip data. At least one set of samples for comparison was labeled with probes that were detected for subsequent analysis. Gene chip results were uploaded to the Gene Expression Omnibus database (serial number: GSE199967).

Bioinformatics analysis of DEGs

Bioinformatics analysis of DEGs was performed as our previous description[34]. DAVID (https://david.ncifcrf.gov/) was used to annotate the functions of the DEGs. STRING (https://string-db.org/) was used to obtain protein-protein interaction (PPI) network. Based on the DEGs interaction data, we used MCC in the CytoHubba plugin to build a hub gene visualization network using Cytoscape (version 3.6.1) software. We used the iRegulon plugin in the Cytoscape (version 3.6.1) software to identify transcription factors (TFs) based on regulatory motifs and chromatin immunoprecipitation sequencing. For ingenuity pathway analysis (IPA; Qiagen, Redwood City, CA, United States), differentially abundant genes were uploaded to IPA for integration analysis, including canonical pathways and molecular interaction networks. The network score was based on a hypergeometric distribution and calculated using the Fisher's exact test *P*-value. The target genes of miRNAs were predicted using TargetScan (http://www.targetscan.org/) software.

Cell culture

The EC cell lines EC9706 and KYSE150 were obtained from the Henan Key Laboratory of TCM Syndrome and Prescription in Signaling, Henan University of Chinese Medicine. EC9706 and KYSE150 cells were cultured in RPMI 1640 (Gibco, CA, United States) supplemented with 10% fetal bovine serum (FBS; Gibco), 100 U/mL penicillin, and 100 mg/mL streptomycin (Sigma-Aldrich, MO, United States) at 37°C in a 5% CO_2 incubator.

Luciferase reporter assay

The 3′-untranslated region (UTR) sequence of *BUB1* mRNA [wild type (WT) or mutant (MUT)] was amplified, cloned, and inserted into a luciferase reporter vector. Then 3′-UTR WT and 3′-UTR MUT vectors were cotransfected with miR-495-3p mimics into EC9706 or KYSE150 cells using Lipofectamine 3000 (Invitrogen, United States). After 48 h, the cells were lysed, and reporter activity was determined using a Dual Luciferase Reporter Assay Kit (Promega, Madison, WI, United States) according to the manufacturer's instructions. The 3′-UTR WT sequence (rmiR495-3p: catttattgtttatgtaaat-GTTTGTTAaaaataaatcccatggaatatttccatgtaac) and 3′-UTR MUT sequence (rmiR495-3p; catttattgtttatgtaaat-CAAACAATaaaataaatcccatggaatatttccatgtaac) were designed and synthesized by Shanghai GenePharma Co., Ltd. (Shanghai, China).

Preparation of Baitouweng decoction aqueous extract

The formulation consisted of *Pulsatillae Radix* (60 g), *Fraxini Cortex* (90 g), *Phellodendri Chinensis Cortex* (90 g), and *Coptidis Rhizoma* (90 g). All above-mentioned herbs were acquired from the Third Affiliated Hospital of Henan University of TCM. Briefly, all herbs were mixed and soaked for 30 min and then boiled in a casserole (1500 mL of distilled water) for 2 h.

Subsequently, the supernatant was centrifuged at 5000 rpm for 30 min, at which point the whole procedure was repeated twice, and the supernatants were mixed together and then evaporated to dryness.

Cell proliferation assay

Cell proliferation was determined using the MTT assay. EC9706 and KYSE150 cells (3000) were seeded in 96-well plates and incubated with Baitouweng decoction (0, 25, 50, 100, 200, 400, and 800μg/mL) for 48 h. After the corresponding treatment, 10 μL of MTT solution was added to each well and incubated for 4 h, and the supernatant was discarded. Then, 150 μL of DMSO was used to detect the absorbance of each well at 570 nm with a microplate analyzer (Thermo Fisher Scientific, United States).

Cell transfection with miRNAs and grouping

siRNA transfection was performed using Lipofectamine 3000 (Invitrogen, Carlsbad, CA, United States) according to the manufacturer's instructions. The study groups were as follows: Control group, NC mimics, Baitouweng, Baitouweng + NC mimics, miR495-3p mimics group, and miR-495-3p mimics + Baitouweng. The sequences of NC mimics (sense: 5′-UUCUCCGAACGUGUCACGUTT-3′; antisense: 5′-ACGUGACACGUUCGGAGAATT-3′) and miR-495-3p mimics (sense: AAACAAACAUGGUGCACUUCUU; antisense: GAAGUGCACCAUGUUUGUUUUU) were designed and synthesized by Shanghai GenePharma Co., Ltd. (Shanghai, China).

Realtime quantitative PCR

Total RNA was extracted from the cell lines using TRIzol reagent (Invitrogen, United States). miRNAs were extracted using the miRNeasy miRNA isolation kit (Qiagen, Germany) according to the manufacturer's protocol. Complementary DNA was synthesized using AMV reverse transcriptase (GIBCO) through reverse transcription. Relative expression levels of target genes were normalized to the endogenous control *GAPDH* or *U6* using the $2^{-\Delta\Delta CT}$ method. Primers for *ABCB1*, *ECT2*, *RALA*, *CDK4*, *ZEB2*, *LOXL2*, *BUB1*, *miR-495-3p*, *GAPDH*, and *U6* were designed and synthesized by Shanghai GenePharma Co., Ltd. (Shanghai, China; Table 1).

Western blot analysis

Proteins were extracted from EC9706 and KYSE105 cells using RIPA buffer containing 1 mmol/L PMSF. Proteins were separated using SDS-PAGE and transferred onto PVDF membranes (Bio-Rad, Hercules, CA, United States). The membranes were blocked with 5% skim milk for 1 h at 25 °C and then incubated with primary antibodies against BUB1 (1:1000; Abcam, Cat. No. ab195268), STAT3 (1:1000; Abcam, Cat. No. ab68153), p-STAT3 (1:5000; Abcam, Cat. No. ab76315), CCNB1 (1:1000; Cell Signaling Technology, Cat. No. 12231), CDK1 (1:5000; Abcam, Cat. No. ab133327), Bax (1:1000; Abcam, Cat. No. ab133327), Caspase3 (1:5000; Abcam, Cat. No. ab32351), Caspase9 (1:1000; Abcam, Cat. No. ab32539), and GAPDH (1:2000; Abcam, Cat. No. ab9485) at 4 °C for 12 h. Blots were then incubated with HRP-conjugated secondary antibodies at 25 °C for 60 min. An enhanced chemiluminescence kit (Thermo Fisher Scientific, United States) was used to visualize the blots, and the intensity of the bands was determined using the ImageJ software (version 1.45; National Institutes of Health, MD, United States).

Cell cycle analysis

Cells were seeded (1×10^6 cells/well) in 100-mm dishes with 10% FBS and incubated overnight at 37 °C in a 5% CO_2 incubator. EC cells were then treated under different conditions (48 h). The cells were collected, incubated in ice-cold 70% ethanol, and fixed overnight at 4 °C. The cells were washed twice with PBS and incubated with 20 mg/mL RNase A and 200 mg/mL propidium iodide (PI) in PBS at room temperature for 30 min in the dark. Finally, a flow cytometer (BD Biosciences, United States) was used for analysis.

Cell apoptosis analysis

To identify apoptotic cells, EC cells were treated under various conditions. After 48 h, Annexin V and PI staining were performed using an Annexin V-fluorescein isothiocyanate Apoptosis Detection kit (Thermo Fisher Scientific, United States). Apoptosis was detected *via* flow cytometry (BD Biosciences).

Wound healing assay

Wound healing assay was performed using EC9706 and KYSE150 cells. Cells were trypsinized, seeded in equal numbers into six-well tissue culture plates, and allowed to grow until confluence (approximately 24 h). Following serum starvation for 24 h, an artificial homogeneous wound (scratch) was created onto the cell monolayer with a sterile 100 μL tip. After scratching, the cells were washed with serum-free medium and complete medium was added, and microscopic images (20 × magnification) of the cells were collected at 0 and 48 h.

Cell invasion assay

The invasion assay was performed using a Transwell chamber, consisting of 8 mm membrane filter inserts coated with Matrigel, and the cells were trypsinized and suspended in serum-free medium. Then, 2×10^4 cells were added to the upper chamber, and the lower chamber was filled with medium containing 10% FBS. After 36 h of incubation, the cells that had invaded the lower chamber were fixed with 4% paraformaldehyde, stained with hematoxylin, and counted under a microscope.

Table 1 Real-time PCR primer sequences

Gene	Sequence
ABCB1	F: 5'-CTTCAGTTACCCATCTCG-3'
	R: 5'- TGGTGGCAAACAATACAG-3'
ECT2	F: 5'-AAGAATGATGGGCACTACCG-3'
	R: 5'-TACTGATGATCTGCCGAGGTC-3'
RALA	F: 5'-ATCGGAAGAAGGTAGTGC-3'
	R: 5'-AAATCTGCTCCCTGAAGT-3'
CDK4	F: 5'-GCCCTCAAGAGTGTGAGAGTC-3'
	R: 5'-CACGAACTGTGCTGATGGGA-3'
ZEB2	F: 5'-GAGGCGCGCGAGAAAGG-3'
	R: 5'-GCCCAGCTTCCCGTAGCC-3'
LOXL2	F: 5'-GTGGATCTGGCACGACTGTCA-3'
	R: 5'-TTGAGCTTCAGCAGGTCATAGTGG-3'
BUB1	F: 5'-GAAAGCATGAGCAATGGGTAAA-3'
	R: 5'-CCACCTGATGCAACTTCTTATG-3'
miR-495-3p	F: 5'-GCGGAAACAAACATGGTGCA-3'
	R: 5'-CAGTGCGTGTCGTGGAGT-3'
GAPDH	F: 5'-GGAGCGAGATCCCTCCAAAAT-3'
	R: 5'-GGCTGTTGTCATACTTCTCATGG-3'
U6	F: 5'-CTCGCTTCGGCAGCACA-3'
	R: 5'-AACGCTTCACGAATTTGCGT-3'

Statistical analysis

GraphPad Prism 8 (GraphPad Software Inc., United States) software was used for data analyses. The data of three independent repeated experiments are expressed as the mean ± SD, and the *t* test was used for comparisons between the two groups. One-way analysis of variance was used for comparison among groups. All P values < 0.05 were considered statistically significant.

RESULTS

Gene chip-based genomic analysis

Based on a database search, 19595 genes were identified. There were 1168 DEGs, of which 614 were upregulated and 554 downregulated. To exhibit the entire expression trend, R software version 3.5.0 (R Foundation for Statistical Computing, Austria) was used to map a volcano plot (Figure 1A). To validate the reliability of the gene chip results, six genes (*ABCB1*, *ECT2*, *RALA*, *CDK4*, *ZEB2*, and *LOXL2*) were subjected to qRT-PCR. The results showed that the six genes had similar expression trends in the gene chip and qRT-PCR (Figure 1B). The results of the PPI network of DEGs are shown in Figure 1C.

Gene Ontology (GO) analysis explained the proteins and important GO terms for biological processes, cellular components, and molecular functions (Figure 2A). IPA showed that the cell cycle control of chromosomal replication, RhoA signaling, and the kinetochore metaphase signaling pathway showed significant changes (Figure 2B). Based on the DEGs interaction data, we used the MCC in the CytoHubba plugin to build a hub gene visualization network in the Cytoscape software, and the results are displayed in Figure 2C. PPI network and hub gene analyses showed that *BUB1*, *TOP2A*, *KIF2C*, and *ASPM* were key node genes. We identified controlled TFs at the beginning of the LR using the iRegulon in Cytoscape. The key enriched TF motivation gene was *HOXD13*, which had a normal enrichment score of 4.085. The changes in the expression of the target genes of *HOXD13* are displayed in color in Figure 2D. The binding motif of *HOXD13* is shown in Figure 2E.

Integrated analysis of differentially abundant genes was performed using the IPA software. In functional and disease analyses, cancer, organismal injury, and abnormalities were identified at the top of the list. In the network function analysis, "amino acid metabolism, molecular transport, organismal" (Figure 3A) were changed significantly, with a score of 44. The "cell morphology, cellular development, cellular growth and proliferation" (Figure 3B) and "cell morphology, cellular assembly and organization, cellular function and maintenance" (Figure 3C) networks were also regarded as key

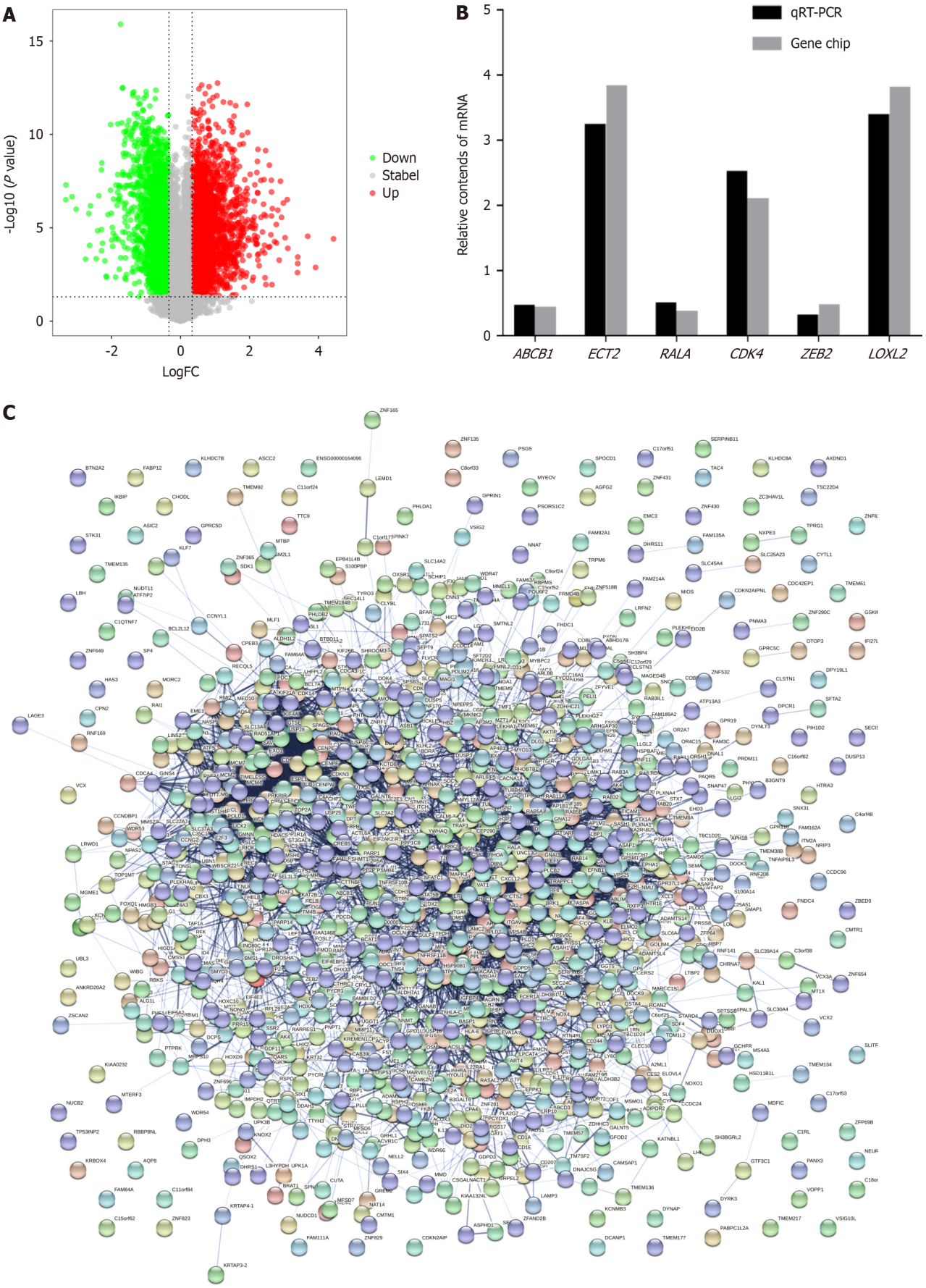

Figure 1 Analysis of differentially expressed genes. A: Volcanic map of differentially expressed genes (DEGs). Red, upregulated; green, downregulated; gray, no significant difference; B: Correlation between genes detected by gene chip and qRT-PCR; C: Protein-protein interaction network for DEGs.

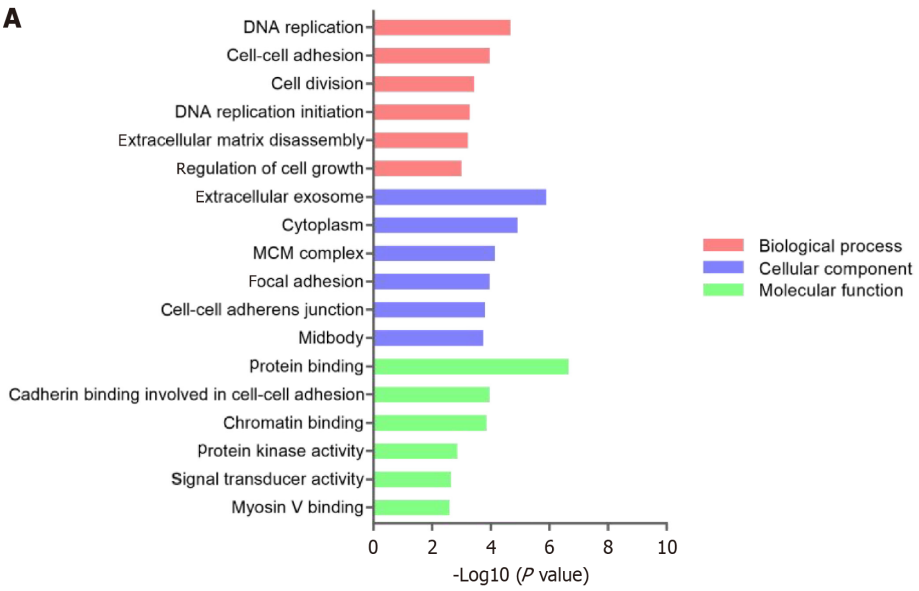
A
DNA replication
Cell-cell adhesion
Cell division
DNA replication initiation
Extracellular matrix disassembly
Regulation of cell growth
Extracellular exosome
Cytoplasm
MCM complex
Focal adhesion
Cell-cell adherens junction
Midbody
Protein binding
Cadherin binding involved in cell-cell adhesion
Chromatin binding
Protein kinase activity
Signal transducer activity
Myosin V binding
0 2 4 6 8 10
-Log10 (P value)
Biological process
Cellular component
Molecular function

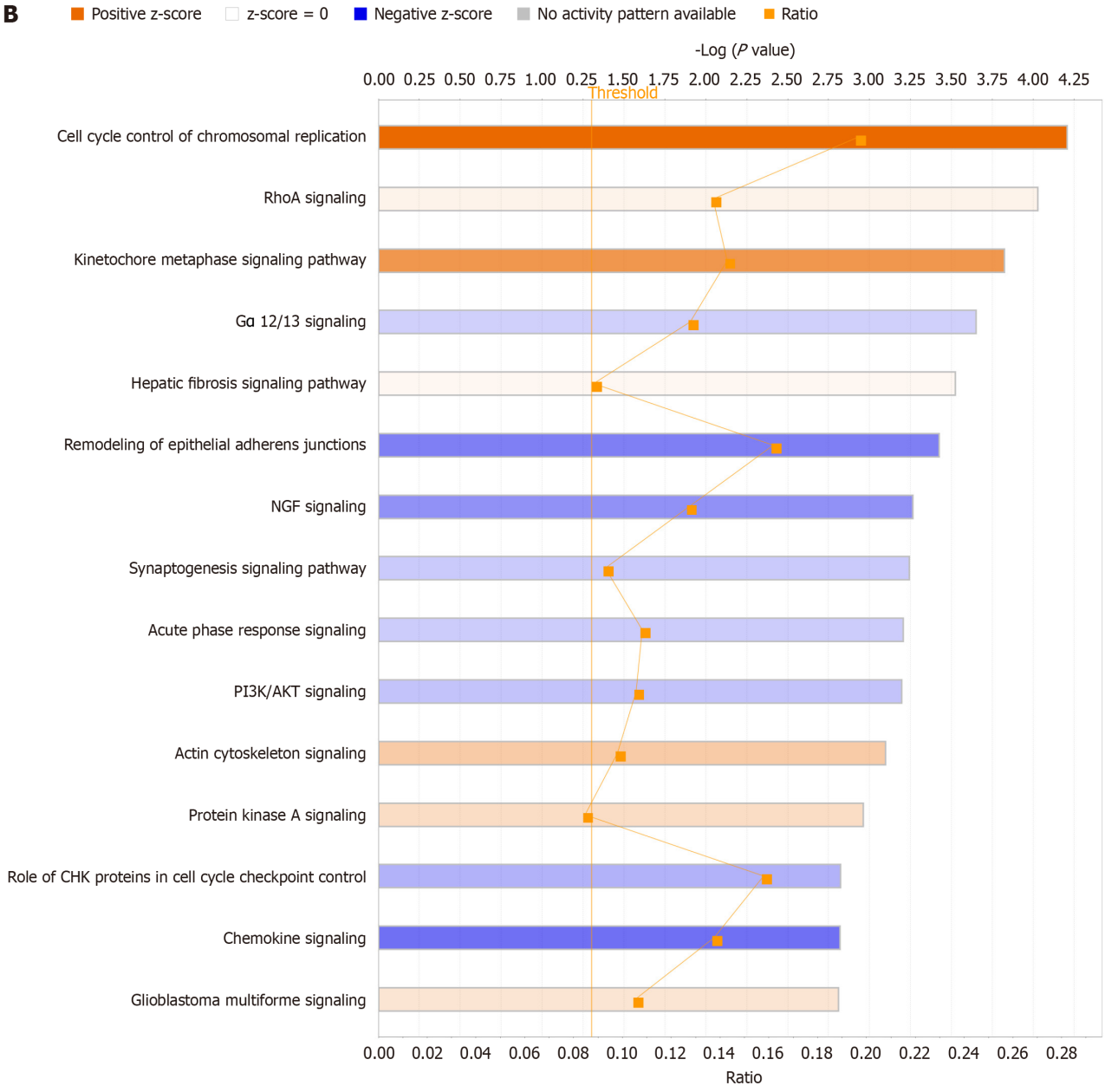
B
Positive z-score
z-score = 0
Negative z-score
No activity pattern available
Ratio
-Log (P value)
0.00 0.25 0.50 0.75 1.00 0.25 1.50 1.75 2.00 2.25 2.50 2.75 3.00 3.25 3.50 3.75 4.00 4.25
Threshold
Cell cycle control of chromosomal replication
RhoA signaling
Kinetochore metaphase signaling pathway
Gα 12/13 signaling
Hepatic fibrosis signaling pathway
Remodeling of epithelial adherens junctions
NGF signaling
Synaptogenesis signaling pathway
Acute phase response signaling
PI3K/AKT signaling
Actin cytoskeleton signaling
Protein kinase A signaling
Role of CHK proteins in cell cycle checkpoint control
Chemokine signaling
Glioblastoma multiforme signaling
0.00 0.02 0.04 0.06 0.08 0.10 0.12 0.14 0.16 0.18 0.20 0.22 0.24 0.26 0.28
Ratio

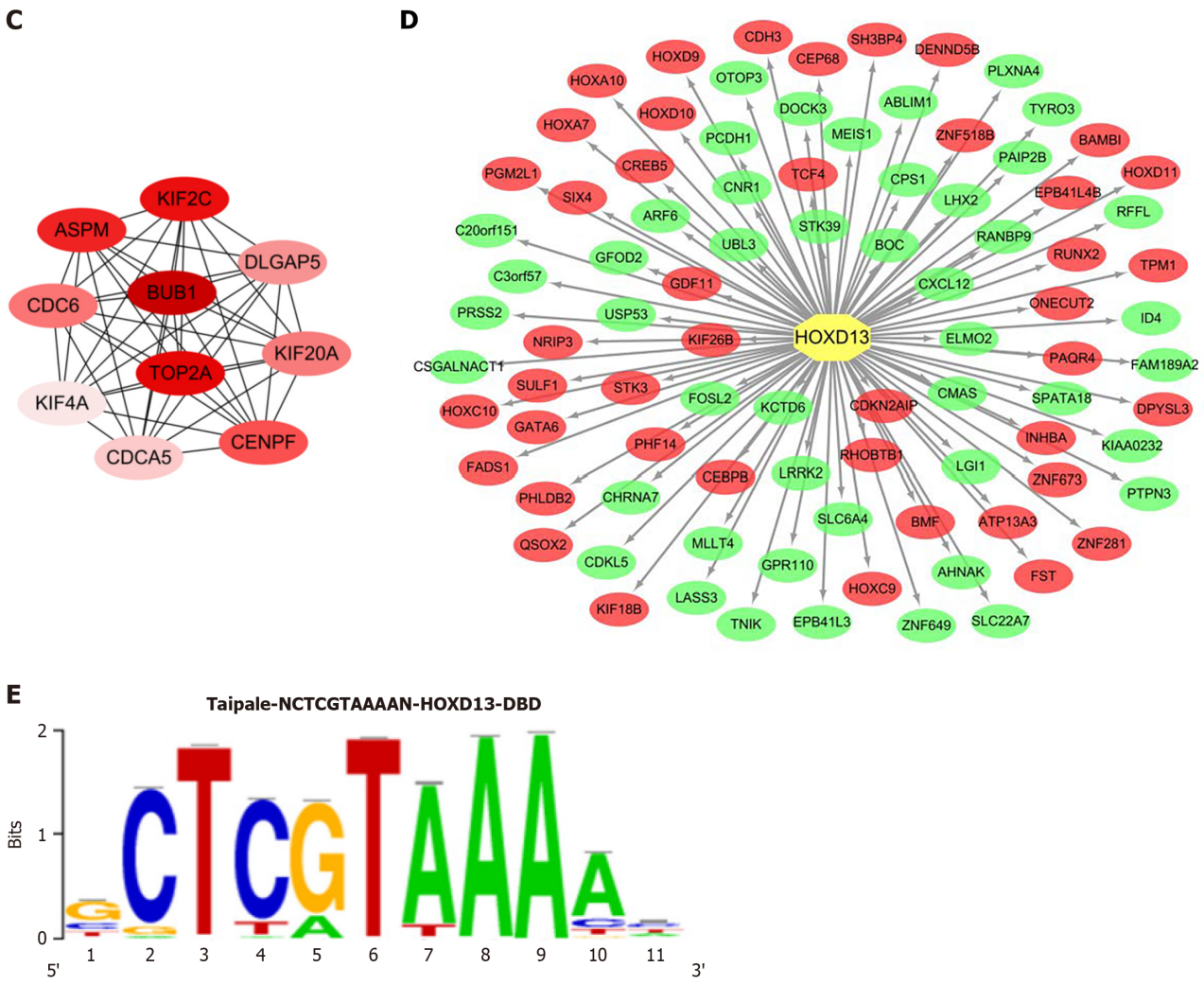

Figure 2 Enrichment analysis of differentially expressed genes. A: Distribution of changed genes in Gene Ontology analysis ($P < 0.05$); B: The canonical pathway of significant change was analyzed with IPA software. Yellow, upward; blue, down; C: Using Cytoscape to describe the hub gene network. The darker the node, the higher the score; D: Target genes of BUB1 predicted using iRegulon in Cytoscape. The nodes in red and green indicate upregulated and downregulated proteins; E: Binding motif of BUB1.

enriched networks as per the transformed products, with scores of 42 and 41, respectively.

Cell proliferation assay

The aqueous extract of Baitouweng decoction was diluted to six concentrations using the concentration ratio dilution method. With increasing concentrations, the inhibitory effect on the proliferation of EC9706 and KYSE150 cells increased (Figure 4A). The half-maximal inhibitory concentration (IC_{50}) of Baitouweng decoction was calculated using the standard curve. The IC_{50} values for EC9706 and KYSE150 cells were 242.8 μg/mL and 164.3 μg/mL, respectively, after 48 h of drug treatment. After the cells were treated with IC_{50} concentrations for 12, 24, 36, 48, and 60 h, the inhibitory effects of the drugs on cell proliferation were calculated. The results indicated that the duration of action and the inhibition rate increased (Figure 4B). The inhibitory effect of Baitouweng decoction on the proliferation of EC cells was dose- and time-dependent.

Bub1 is the target gene of miR-495-3p

The results of prediction based on the TargetScan database showed that mi-495-3p has a specific binding site in the *BUB1* mRNA 3'-UTR (Figure 5A), indicating that it is possible for mi-495-3p to target and regulate BUB1. To verify the prediction, we constructed luciferase reporter genes of wild-type and mutant BUB1-3′-UTR. The results showed that the dual luciferase activity in the BUB1-3′-UTR-WT + miR-495-3p group was significantly lower than that in the BUB1-3′-UTR-WT + NC group. There was no significant difference in double luciferase activity between the BUB1-3′-UTR-MUT + miR-495-3p and the BUB1-3′-UTR-MUT + NC groups (Figure 5B and C). It was confirmed that *BUB1* is a target gene of miR-495-3p.

Baitouweng decoction inhibits BUB1 expression

qRT-PCR analysis showed that Baitouweng decoction significantly downregulated *BUB1* mRNA levels in the EC cell lines

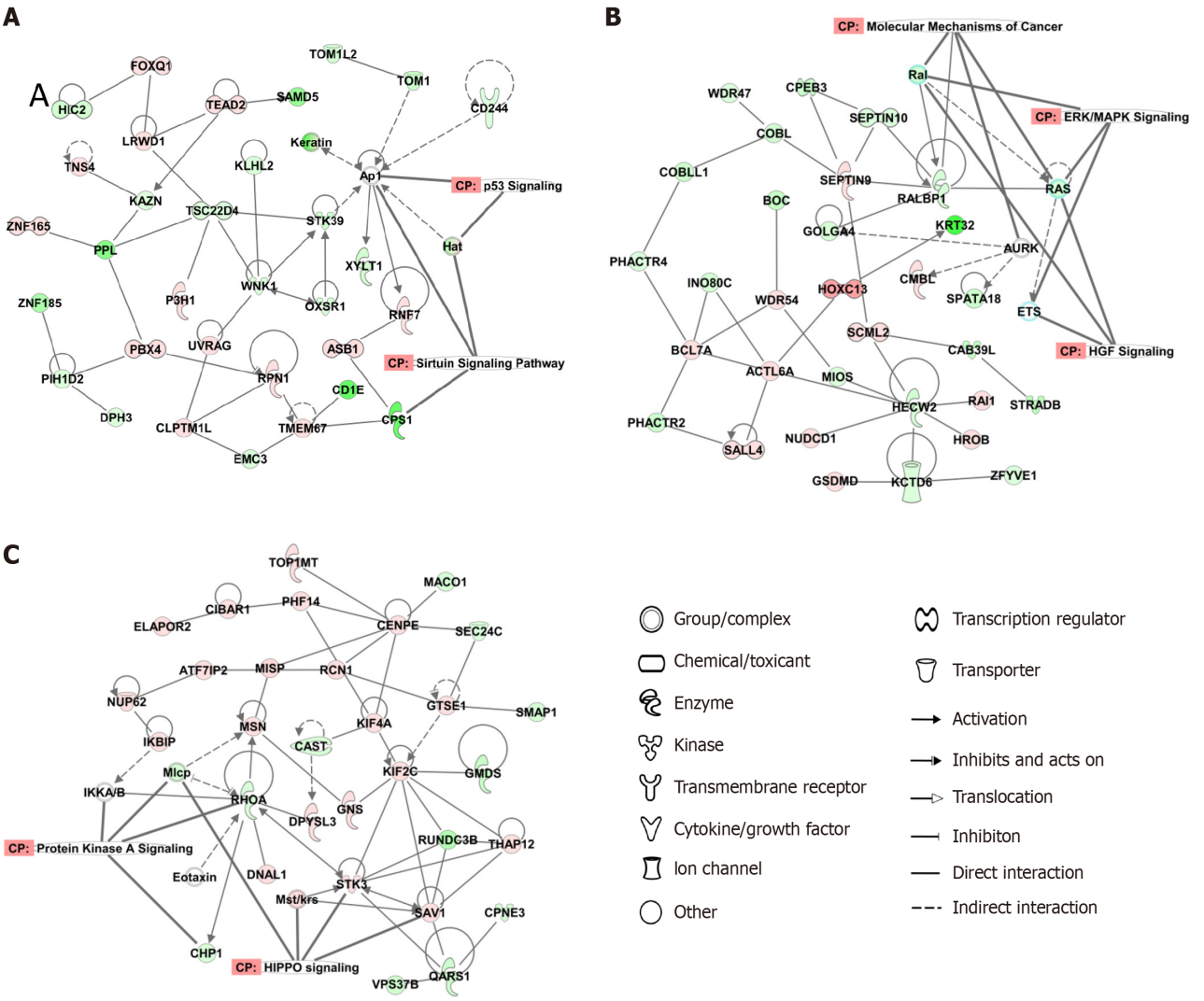

Figure 3 Ingenuity pathway analysis. A–C: Top-ranked enriched networks based on differentially abundant genes. Red, increased; green, decreased.

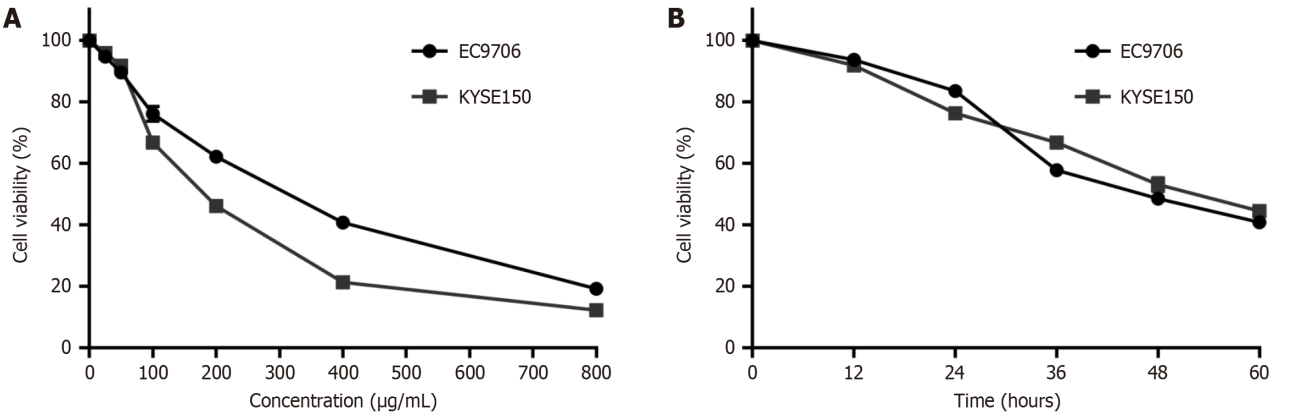

Figure 4 Baitouweng decoction inhibits proliferation of esophageal cancer cells in a dose- and time-dependent manner. A: Dose-effect relationship of Baitouweng decoction on esophageal cancer cells; B: Time-effect relationship of Baitouweng decoction on esophageal cancer cells.

EC9706 and KYSE150 (Figure 6A). Western blot analysis showed that Baitouweng decoction significantly inhibited BUB1 protein expression (Figure 6B). Baitouweng decoction or miR495-3p mimics significantly upregulated the expression of miR-495-3p in EC9706 and KYSE150 cells (Figure 6C).

Effect of Baitouweng decoction on cell cycle and apoptosis

Cell cycle analysis showed that after treatment with Baitouweng decoction, both EC9706 (Figure 7A) and KYSE150

A **Conserved**

	Predicted consequential pairing of target region (top) and miRNA (bottom)	Site type	Context++ score	Context++ score percentile	Weighted context++ score	Conserved branch length	P_{CT}	Predicted relative K_D
Position 94-101 of BUB1 3' UTR	5' ...AUUGUUUAUGUAAAUGUUUGUUA...	8mer	-0.34	99	-0.29	1.915	N/A	-5.855
hsa-miR-495-3p	3' UUCUUCACGUGGUACAAACAAA							

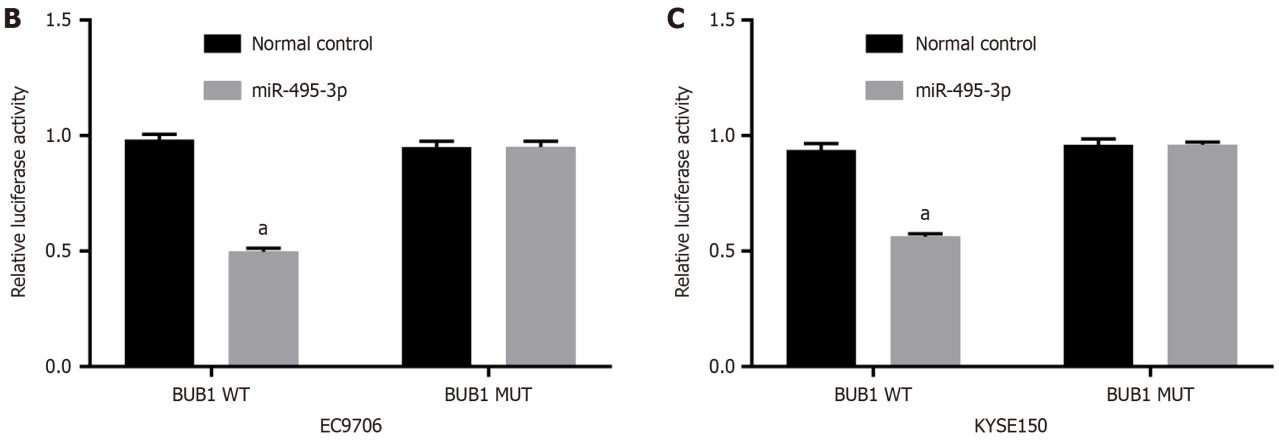

Figure 5 *BUB1* is a target gene of miR-495-3p. A: Diagram of the putative binding sites of miR-495-3p in the 3'-untranslated regions of BUB1; B and C: Dual luciferase activity in EC9706 cells and KYSE150 cells. [a]*P* < 0.01 compared with normal control. UTR: Untranslated region; WT: Wild type; MUT: Mutant.

(Figure 7B) cells showed obvious cell arrest in the G2/M phase. Baitouweng decoction induced apoptosis in EC9706 and KYSE150 cells (Figure 7C and D).

Baitouweng decoction inhibits EC cell migration and invasion

To investigate the biological significance of Baitouweng decoction in EC, we examined its effects on the migration and invasion of EC cells. Wound healing assay showed that Baitouweng decoction or miR-495-3p mimics significantly reduced the number of migrating EC9706 and KYSE150 cells (Figure 8A and B). Transwell assay with Matrigel showed that Baitouweng decoction led to a significant decrease in the invasive potential of EC9706 and KYSE150 cells (Figure 8C and D). In summary, Baitouweng decoction inhibited EC migration and invasion.

Protein expression of STAT3, p-STAT3, CCNB1 CDK1, Bax, Caspase3, and Caspase9 in different groups

To further explore the effect of Baitouweng decoction on EC cells, we analyzed the expression levels of several key proteins following the treatment of EC9706 and KYSE150 cells with Baitouweng decoction for 48 h. We found that the expression levels of apoptosis-related proteins (Bax, Caspase 3, and Caspase 9) in the Baitouweng decoction and miR-495-3p mimics groups were upregulated. Western blot analysis was then performed to examine the expression levels of key cell cycle regulators (G2/M), including CCNB1 and CDK1. The formation of the CCNB1/CDK1 complex is essential for the G2/M transition. Baitouweng decoction and miR-495-3p mimics significantly downregulated the expression of the p-STAT3 protein, but the total protein expression of STAT3 showed no significant change (Figure 9).

DISCUSSION

In our study, 1168 DEGs were identified, of which 614 were upregulated and 554 downregulated. GO enrichment analysis revealed that most proteins are related to DNA replication, cell-cell adhesion, and cell division. Canonical pathway analysis based on the DEGs showed that most of these genes are involved in cell cycle regulation of chromosomal replication, RhoA signaling, kinetochore metaphase signaling pathway, and Gα12/13 signaling. Genomic analysis using the IPA network showed that variations in DEGs are related to "cell morphology, development, growth, and proliferation". These biological processes, signaling pathways, and networks are primarily related to mitosis. These results are consistent with previous studies[35].

PPI and hub gene analyses showed that *BUB1*, *TOP2A*, *KIF2C*, *ASPM*, and *CENPF* were key node genes, with *BUB1* having the highest score. They are also involved in cell-cycle regulation. Cell division occurs during the cell cycle. However, the loss of control over cell division leads to endless growth and proliferation of cells, eventually becoming a cancer marker[36]. Base excision repair is a key pathway in genome maintenance and has a tumor-inhibiting effect. BUB1 is a spindle-checkpoint protein[37]. It is essential for spindle assembly checkpoint signaling and correct chromosomal alignment. It plays a key role in the assembly of checkpoint proteins at the kinetochore and is required for the subsequent localization of CENPF, BUB1B, CENPE, and MAD2L1[38]. The BUB1-BUB3 complex plays a role in the inhibition of APC/C when the spindle assembly checkpoint is activated and inhibits the ubiquitin ligase activity of APC/C by phosphorylating its activator CDC20. This complex also phosphorylates MAD1L1. Kinase activity is essential for the

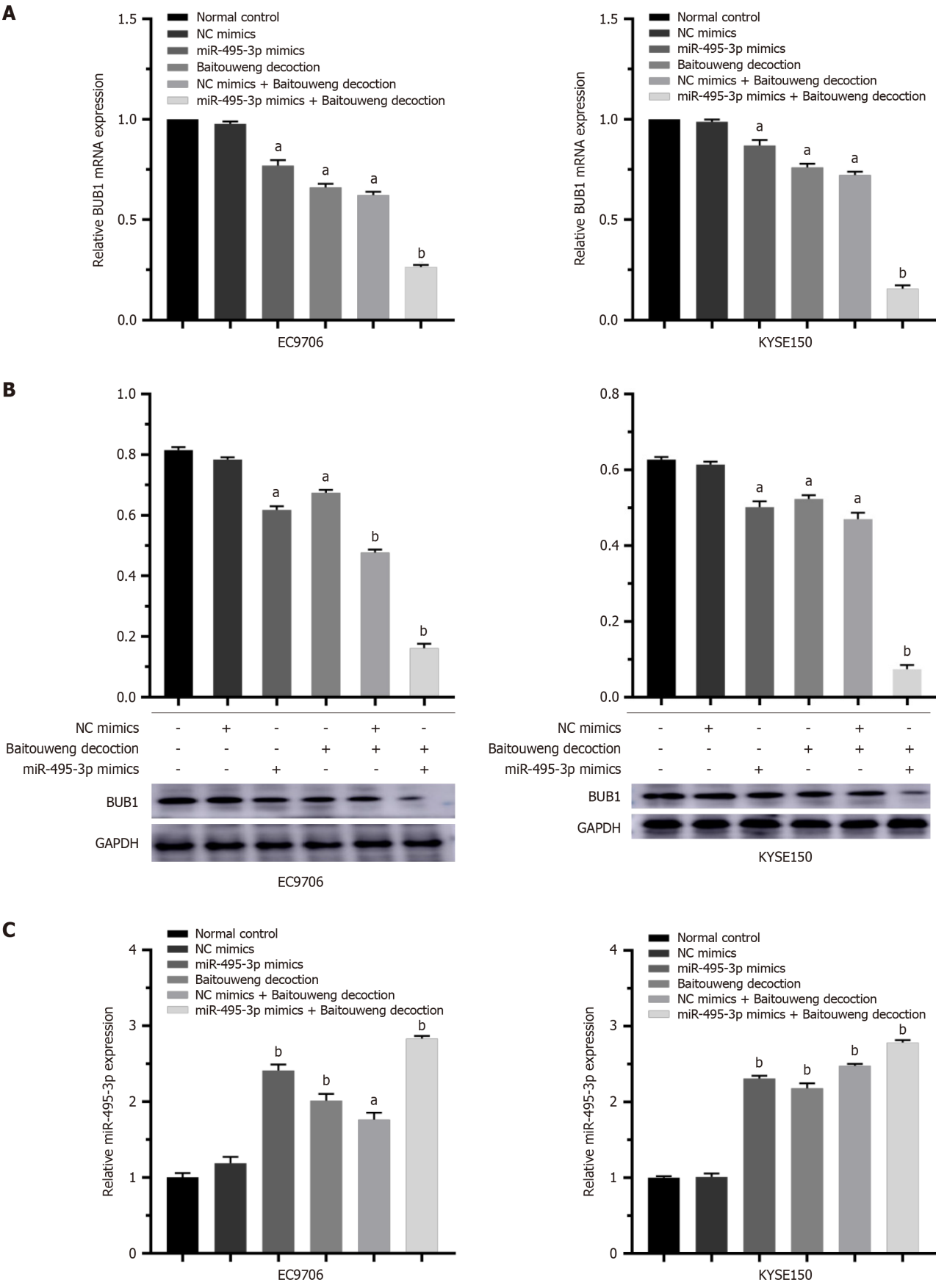

Figure 6 Baitouweng decoction inhibits BUB1 expression. A: qRT-PCR analysis of the effect of Baitouweng decoction on the expression of *BUB1* in EC9706 and KYSE150 cells; B: Western blot analysis of Baitouweng decoction on the expression of BUB1 in EC9706 and KYSE150 cells; C: Baitouweng decoction or miR495-3p mimics significantly upregulate the expression of miR-495-3p in EC9706 and KYSE150 cells. $^{a}P < 0.05$, $^{b}P < 0.01$ compared with normal control.

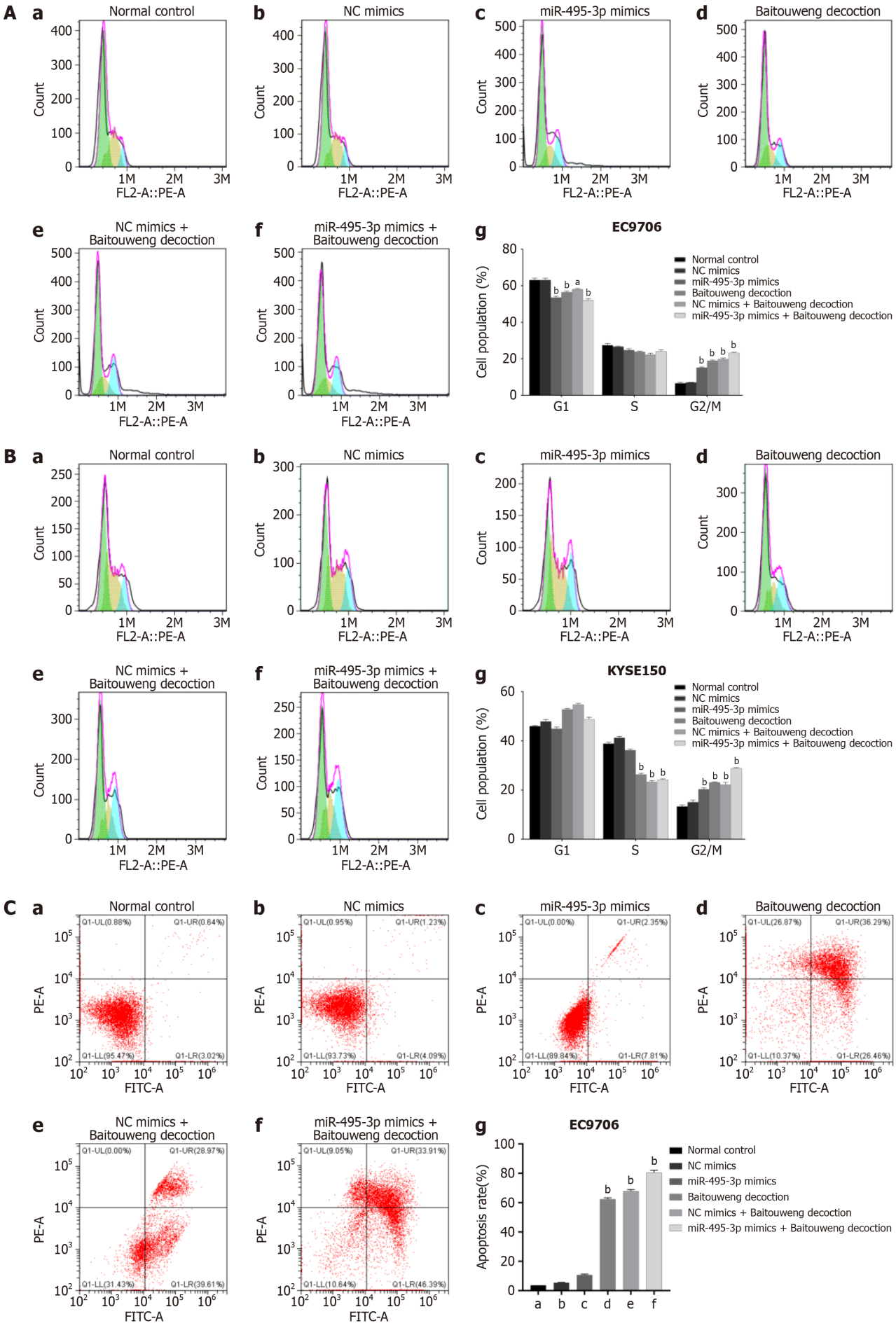
A
a Normal control
b NC mimics
c miR-495-3p mimics
d Baitouweng decoction
e NC mimics + Baitouweng decoction
f miR-495-3p mimics + Baitouweng decoction
g EC9706
Count
FL2-A::PE-A
Cell population (%)
G1
S
G2/M
Normal control
NC mimics
miR-495-3p mimics
Baitouweng decoction
NC mimics + Baitouweng decoction
miR-495-3p mimics + Baitouweng decoction
B
a Normal control
b NC mimics
c miR-495-3p mimics
d Baitouweng decoction
e NC mimics + Baitouweng decoction
f miR-495-3p mimics + Baitouweng decoction
g KYSE150
C
a Normal control
b NC mimics
c miR-495-3p mimics
d Baitouweng decoction
e NC mimics + Baitouweng decoction
f miR-495-3p mimics + Baitouweng decoction
g EC9706
PE-A
FITC-A
Apoptosis rate(%)

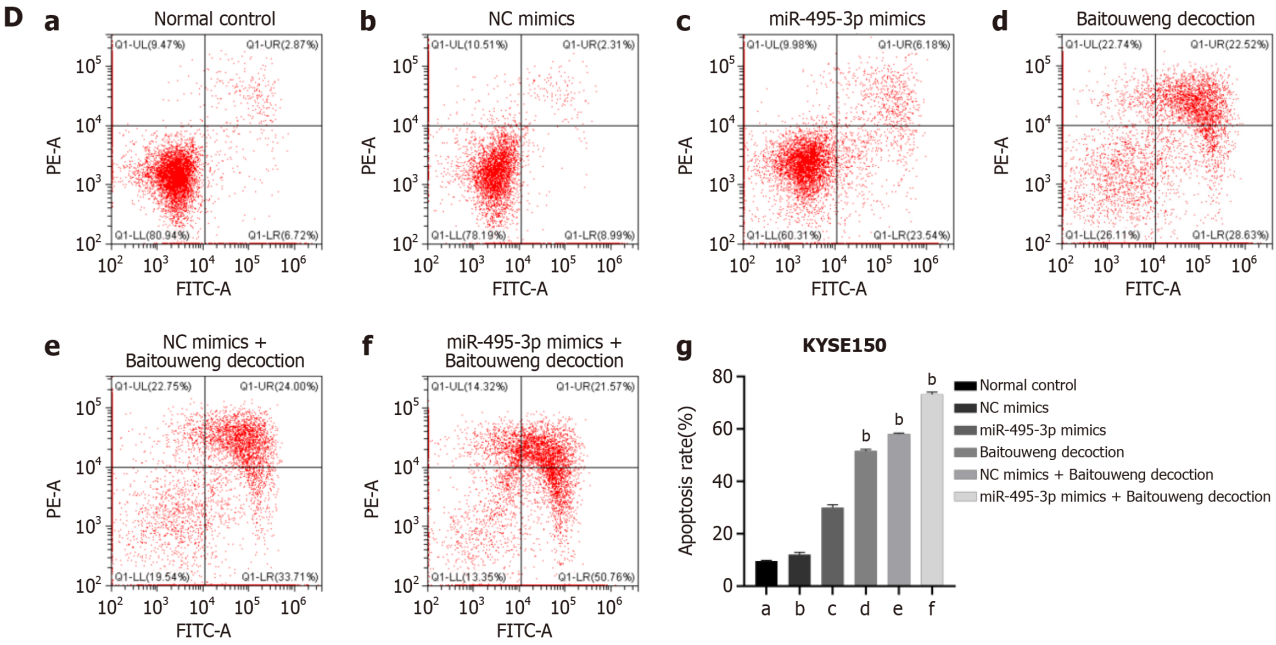

Figure 7 Effect of Baitouweng decoction on the cell cycle and apoptosis of esophageal cancer cells. A and B: Baitouweng decoction induces G2/M phase arrest in EC9706 and KYSE150 cells; C and D: Baitouweng decoction increases the apoptosis of EC9706 and KYSE150 cells. $^{a}P < 0.05$, $^{b}P < 0.01$ compared with normal control.

inhibition of APC/CCDC20 and chromosome alignment, but does not play a major role in spindle assembly checkpoint activity[39]. BUB1 mediates cell death and inhibits spontaneous tumorigenesis, which may play a role in the DNA damage response, and the mutation of this gene is related to aneuploidy[40]. In our study, Baitouweng decoction inhibited the expression of BUB1. Low BUB1 expression inhibits the proliferation, invasion, and migration of tumor cells, decreases cell viability, and increases cell apoptosis[41,42]. The expression level of BUB1 may be related to the occurrence, development, and lymph node metastasis of esophageal squamous cell carcinoma[43]. However, its mechanism of action requires further investigation.

TCM prescriptions play an essential role in the treatment of tumors. Over the past 20 years, our team has found that Qigesan, Tongyou, Xiaoxianxiong, and Shashenmaidong decoctions inhibit esophageal cancer cell proliferation and tumor growth. We continued to explore the treatment of esophageal cancer. Searching the literature, it was found that Baitouweng decoction is mostly used in the treatment of colitis[44-47]. The main pathogeneses of EC are deficiency, stagnation, phlegm, and fire. During the pathological evolution of EC, depressed qi transforms into fire, phlegm, and blood stasis. At this time, there also can be evil heat and poison. It has some similarities with Baitouweng decoction in treating damp-heat and stasis-toxin. The treatment of EC with Baitouweng decoction can be classified into the category of the same treatment for different diseases in TCM. The application of Baitouweng decoction in the prevention and treatment of EC has a theoretical basis. In this study, Baitouweng inhibited EC cell activity in a time- and dose-dependent manner.

Increasing evidence has shown that miRNAs are important regulators of various cellular processes. In recent years, it has been widely studied in the occurrence and development of EC[48-51]. In this study, we used the Target Scan database to predict that mi-495-3p has a specific binding site in *BUB1* mRNA 3′-UTR. Furthermore, using dual-luciferase reporter assay, we confirmed that *BUB1* is a target gene of miR-495-3p. miR-495 is a noncoding RNA located at 14q32.31 site on the human chromosome. It has been reported that miR-495-3p has anticancer effects in various cancers[52-54]. Our analysis showed that Baitouweng decoction and overexpression of miR-495-3p significantly downregulated the mRNA and protein expression levels of BUB1, whereas Baitouweng decoction upregulated the expression level of miR-495-3p. Induction of apoptosis in cancer cells is a key therapeutic strategy for cancer treatment. In this study, we found that Baitouweng decoction and miR-495-3p significantly induced apoptosis of esophageal cancer cells. Bax, Caspase 3, and Caspase 9 were upregulated by Baitouweng decoction, which induced EC cell apoptosis. These results suggest that Baitouweng decoction may induce apoptosis by upregulating the expression of miR-495-3p. The cell cycle is a complex process. We found that Batouweng decoction induced G2/M phase arrest. BUB1, CCNB1, and CDK1 play important roles during the G2/M transition and M phase. BUB1 promotes cancer cell proliferation by promoting G2/M transition in the cell cycle[55]. Decreased CCNB1/CDK1 expression leads to G2/M arrest[56]. In our study, the downregulated expression of BUB1, CCNB1, and CDK1 reduced the transformation of cells from the G2/M to M phase, which is consistent with the results of previous studies[57,58].

STAT3 is a signal transducer and activator of transcription. STAT3 is abnormally activated in many types of malignant tumors and is involved in the biological processes of cancer cell proliferation, apoptosis, and invasion[59,60]. High p-STAT3 expression is an important factor in the malignant phenotype of EC. Inhibition of the STAT3 signaling pathway can significantly inhibit the malignant phenotype of EC[61]. Curcumin exerts its anti-tumor action by inhibiting the

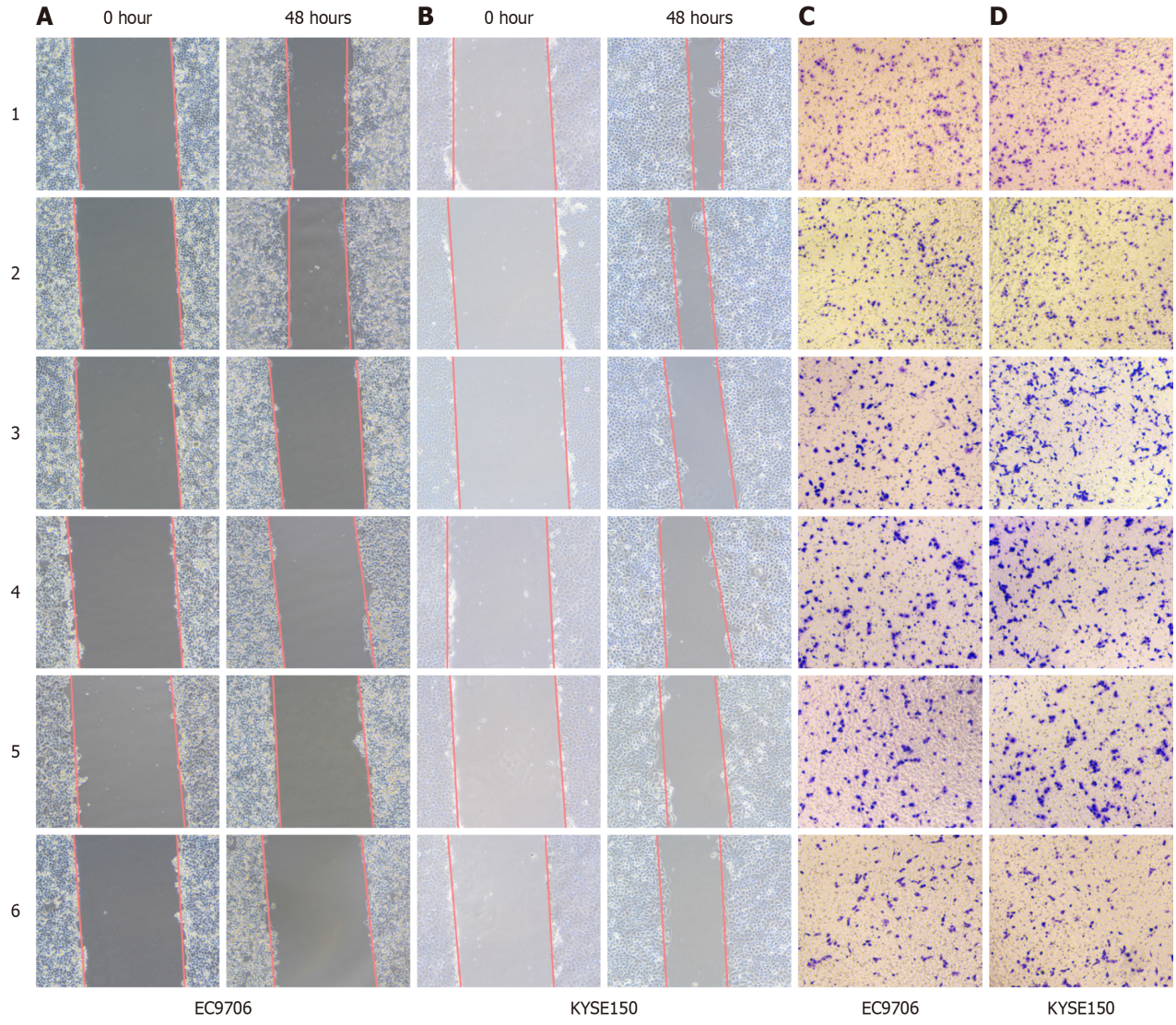

Figure 8 Effect of Baitouweng decoction on migration and invasion of esophageal cancer cells. A and B: Baitouweng decoction reduces the migration activity of both EC9706 and KYSE150 cells; C and D: Baitouweng decoction reduce the invasion activity of both EC9706 and KYSE150 cells. 1: Normal control; 2: NC mimics; 3: miR-495-3p mimics; 4: Baitouweng decoction; 5: NC mimics + Baitouweng decoction; 6: miR-495-3p mimics + Baitouweng decoction.

STAT3 signaling pathway, and the STAT3 pathway appears to be an effective target for EC. We identified the transcription factor STAT3 as a new BUB1 substrate and verified that BUB1 directly regulates transcription. Thus, BUB1 is essential for STAT3 phosphorylation[62]. We found that Baitouweng decoction or miR-495-3p mimics decreased the expression of p-STAT3 in EC9706 and KYSE150 cells but did not decrease the expression level of total STAT3. Baitouweng decoction effectively inhibited STAT3 phosphorylation and STAT3-mediated transactivation in EC cells by downregulating BUB1. STAT3 is phosphorylated in ovarian, cervical, and endometrial cancers[63-65]. Currently, targeted tumor therapy can be achieved by directly or indirectly blocking STAT3[66,67]. STAT3 blocking therapy may be a new direction for tumor therapy.

CONCLUSION

In summary, we analyzed DEGs in esophageal cancer using bioinformatics and found that these gene changes were related to mitosis. We also found that miR-495-3p directly targeted BUB1 and inhibited BUB1 expression. Baitouweng decoction inhibited the activity of esophageal cancer cells. We also explored the mechanism of action of Baitouweng decoction in EC cells. The results showed that Baitouweng decoction inhibited the proliferation, migration, and invasion of EC cells, interfered with the cell cycle of esophageal cancer cells, and induced apoptosis. Baitouweng decoction inhibits the growth of esophageal cancer cells probably through miR-495-3p targeting the BUB1-mediated STAT3 signaling pathway. Therefore, this information may aid in the development of novel EC treatments.

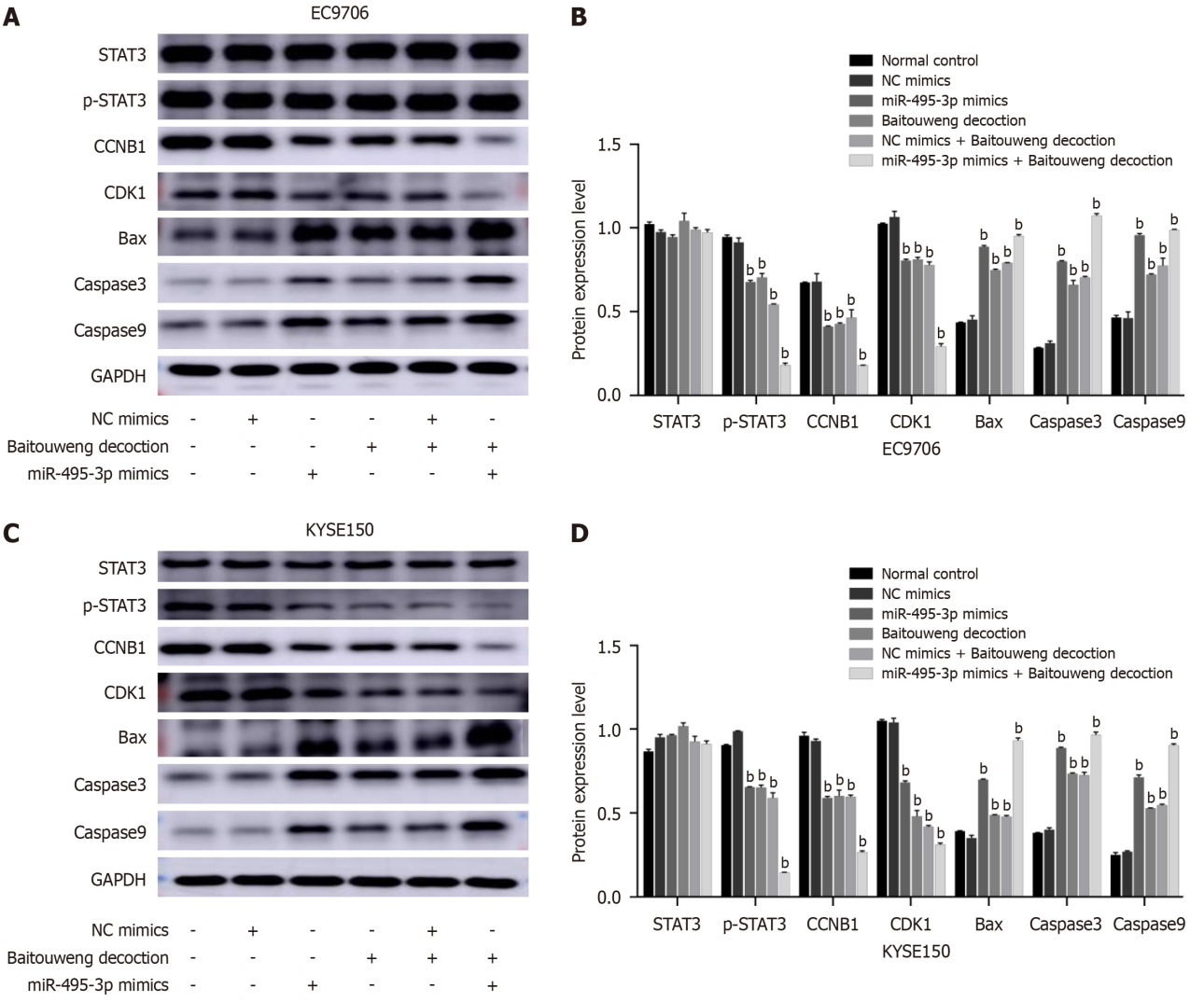

Figure 9 Protein expression of STAT3, p-STAT3, CCNB1, CDK1, Bax, Caspase3, and Caspase9 in different groups detected using Western blot. A and B: EC9706 cells; C and D: KYSE150 cells. $^{b}P < 0.01$ compared with normal control.

FOOTNOTES

Author contributions: Yang H wrote the manuscript and analyzed the data; Si FC participated in the study design and interpretation; Chen XW and Yang H performed the experiments; Song XJ and Du HY acquired and analyzed the data; all the authors have read and approved the final manuscript.

Supported by National Natural Science Foundation of China, No. 81550014; Henan Provincial Science and Technology Research Project, No. 222102310187 and No. 242102310582; and Henan Province Postdoctoral Research Project, No. 202103092.

Institutional review board statement: The study was reviewed and approved by The First Affiliated Hospital of Henan University of Chinese Medicine.

Conflict-of-interest statement: The authors declare that they have no competing interests to disclose.

Data sharing statement: Technical appendix, statistical code, and dataset are available from the corresponding author at sifc2000@hotmail.com.

Country of origin: China

ORCID number: Hui Yang 0000-0002-5286-0956; Fu-Chun Si 0000-0002-9880-7333.

S-Editor: Lin C
L-Editor: Wang TQ
P-Editor: Zheng XM

REFERENCES

1 **Xia C**, Dong X, Li H, Cao M, Sun D, He S, Yang F, Yan X, Zhang S, Li N, Chen W. Cancer statistics in China and United States, 2022: profiles, trends, and determinants. *Chin Med J (Engl)* 2022; **135**: 584-590 [PMID: 35143424 DOI: 10.1097/CM9.0000000000002108]
2 **Mönig S**, Chevallay M, Niclauss N, Zilli T, Fang W, Bansal A, Hoeppner J. Early esophageal cancer: the significance of surgery, endoscopy, and chemoradiation. *Ann N Y Acad Sci* 2018; **1434**: 115-123 [PMID: 30138532 DOI: 10.1111/nyas.13955]
3 **Sheikh M**, Roshandel G, McCormack V, Malekzadeh R. Current Status and Future Prospects for Esophageal Cancer. *Cancers (Basel)* 2023; **15** [PMID: 36765722 DOI: 10.3390/cancers15030765]
4 **Blum Murphy MA**, Elimova E, Ajani JA. Current concepts and future potential in neoadjuvant chemotherapy for esophageal cancer. *Expert Rev Gastroenterol Hepatol* 2016; **10**: 383-392 [PMID: 26560689 DOI: 10.1586/17474124.2016.1116936]
5 **Imazeki H**, Kato K. Development of chemotherapeutics for unresectable advanced esophageal cancer. *Expert Rev Anticancer Ther* 2020; **20**: 1083-1092 [PMID: 32820965 DOI: 10.1080/14737140.2020.1814149]
6 **Smyth EC**, Lagergren J, Fitzgerald RC, Lordick F, Shah MA, Lagergren P, Cunningham D. Oesophageal cancer. *Nat Rev Dis Primers* 2017; **3**: 17048 [PMID: 28748917 DOI: 10.1038/nrdp.2017.48]
7 **Huang FL**, Yu SJ. Esophageal cancer: Risk factors, genetic association, and treatment. *Asian J Surg* 2018; **41**: 210-215 [PMID: 27986415 DOI: 10.1016/j.asjsur.2016.10.005]
8 **Feng XY**, Chen BC, Li JC, Li JM, Li HM, Chen XQ, Liu D, Li RT. Gansui-Banxia Decoction extraction inhibits MDSCs accumulation *via* AKT /STAT3/ERK signaling pathways to regulate antitumor immunity in C57bl/6 mice. *Phytomedicine* 2021; **93**: 153779 [PMID: 34638030 DOI: 10.1016/j.phymed.2021.153779]
9 **Jiang JH**, Pi J, Jin H, Yang F, Cai JY. Chinese herb medicine matrine induce apoptosis in human esophageal squamous cancer KYSE-150 cells through increasing reactive oxygen species and inhibiting mitochondrial function. *Pathol Res Pract* 2018; **214**: 691-699 [PMID: 29567333 DOI: 10.1016/j.prp.2018.03.015]
10 **Li Z**, Feiyue Z, Gaofeng L. Traditional Chinese medicine and lung cancer--From theory to practice. *Biomed Pharmacother* 2021; **137**: 111381 [PMID: 33601147 DOI: 10.1016/j.biopha.2021.111381]
11 **Guo YM**, Huang YX, Shen HH, Sang XX, Ma X, Zhao YL, Xiao XH. Efficacy of Compound Kushen Injection in Relieving Cancer-Related Pain: A Systematic Review and Meta-Analysis. *Evid Based Complement Alternat Med* 2015; **2015**: 840742 [PMID: 26504481 DOI: 10.1155/2015/840742]
12 **Wang Y**, Zhang Q, Chen Y, Liang CL, Liu H, Qiu F, Dai Z. Antitumor effects of immunity-enhancing traditional Chinese medicine. *Biomed Pharmacother* 2020; **121**: 109570 [PMID: 31710893 DOI: 10.1016/j.biopha.2019.109570]
13 **Hua YL**, Ma Q, Zhang XS, Jia YQ, Peng XT, Yao WL, Ji P, Hu JJ, Wei YM. Pulsatilla Decoction Can Treat the Dampness-Heat Diarrhea Rat Model by Regulating Glycerinphospholipid Metabolism Based Lipidomics Approach. *Front Pharmacol* 2020; **11**: 197 [PMID: 32194420 DOI: 10.3389/fphar.2020.00197]
14 **Niu C**, Hu XL, Yuan ZW, Xiao Y, Ji P, Wei YM, Hua YL. Pulsatilla decoction improves DSS-induced colitis *via* modulation of fecal-bacteria-related short-chain fatty acids and intestinal barrier integrity. *J Ethnopharmacol* 2023; **300**: 115741 [PMID: 36162543 DOI: 10.1016/j.jep.2022.115741]
15 **Liu Y**, Zhou M, Yang M, Jin C, Song Y, Chen J, Gao M, Ai Z, Su D. Pulsatilla chinensis Saponins Ameliorate Inflammation and DSS-Induced Ulcerative Colitis in Rats by Regulating the Composition and Diversity of Intestinal Flora. *Front Cell Infect Microbiol* 2021; **11**: 728929 [PMID: 34804990 DOI: 10.3389/fcimb.2021.728929]
16 **Liu H**, Hu Y, Qi B, Yan C, Wang L, Zhang Y, Chen L. Network pharmacology and molecular docking to elucidate the mechanism of pulsatilla decoction in the treatment of colon cancer. *Front Pharmacol* 2022; **13**: 940508 [PMID: 36003525 DOI: 10.3389/fphar.2022.940508]
17 **Hua YL**, Ma Q, Li W, Zhang XS, Cheng XH, Jia YQ, Peng XT, Yao WL, Ji P, Hu JJ, Wei YM. Metabolomics analysis of Pulsatilla decoction on treatment of wetness-heat-induced diarrhea in rats based on UPLC-Q/TOF-MS/MS. *Biomed Chromatogr* 2019; **33**: e4629 [PMID: 31242331 DOI: 10.1002/bmc.4629]
18 **Lin MK**, Yang YT, Lin LJ, Yu WH, Chen HY. Pulsatilla decoction suppresses matrix metalloproteinase-7-mediated leukocyte recruitment in dextran sulfate sodium-induced colitis mouse model. *BMC Complement Med Ther* 2022; **22**: 211 [PMID: 35933374 DOI: 10.1186/s12906-022-03696-w]
19 **Liu F**. The influence of prescriptions in Treatise on Febrile Diseases on the biological characteristics of esophageal carcinoma cell lines TE-1, EC-1, EC109 and EC9706. M.Sc. Thesis, Henan University of Traditional Chinese Medicine. 2018. Available from: https://kns.cnki.net/kcms2/article/abstract?v=8dkf_uZKVx1qCAnhBx9dsh9fWUIHc-4UkzbOa2oli_Vm3YZJVxjieRS-QbMZCbxqQZadt4-WyKI_kuOlu5rwb09vz8AsddhPZuDOY_Pas-ok4EQjKIcOnVMldYvX5KZhBx7DaZed1E4pORo-YdtO4A==&uniplatform=NZKPT&language=CHS
20 **Jiang SY**. Effects of Three Heat-clearing Prescriptions from Treatise on Febrile Diseases on the Proliferation, Apoptosis and EGFR-PLC-γ1 Protein Phosphorylation in Human Esophageal Carcinoma Cells. M.Sc. Thesis, Henan University of Traditional Chinese Medicine. 2021
21 **Singh P**, Pesenti ME, Maffini S, Carmignani S, Hedtfeld M, Petrovic A, Srinivasamani A, Bange T, Musacchio A. BUB1 and CENP-U, Primed by CDK1, Are the Main PLK1 Kinetochore Receptors in Mitosis. *Mol Cell* 2021; **81**: 67-87.e9 [PMID: 33248027 DOI: 10.1016/j.molcel.2020.10.040]
22 **Han JY**, Han YK, Park GY, Kim SD, Lee CG. Bub1 is required for maintaining cancer stem cells in breast cancer cell lines. *Sci Rep* 2015; **5**: 15993 [PMID: 26522589 DOI: 10.1038/srep15993]
23 **Li M**, Duan X, Xiao Y, Yuan M, Zhao Z, Cui X, Wu D, Shi J. BUB1 Is Identified as a Potential Therapeutic Target for Pancreatic Cancer Treatment. *Front Public Health* 2022; **10**: 900853 [PMID: 35769782 DOI: 10.3389/fpubh.2022.900853]
24 **Tong H**, Wang J, Chen H, Wang Z, Fan H, Ni Z. Transcriptomic analysis of gene expression profiles of stomach carcinoma reveal abnormal expression of mitotic components. *Life Sci* 2017; **170**: 41-49 [PMID: 27923621 DOI: 10.1016/j.lfs.2016.12.001]

25 **Zhu LJ**, Pan Y, Chen XY, Hou PF. BUB1 promotes proliferation of liver cancer cells by activating SMAD2 phosphorylation. *Oncol Lett* 2020; **19**: 3506-3512 [PMID: 32269624 DOI: 10.3892/ol.2020.11445]

26 **Jiang N**, Liao Y, Wang M, Wang Y, Wang K, Guo J, Wu P, Zhong B, Guo T, Wu C. BUB1 drives the occurrence and development of bladder cancer by mediating the STAT3 signaling pathway. *J Exp Clin Cancer Res* 2021; **40**: 378 [PMID: 34852826 DOI: 10.1186/s13046-021-02179-z]

27 **Ali Syeda Z**, Langden SSS, Munkhzul C, Lee M, Song SJ. Regulatory Mechanism of MicroRNA Expression in Cancer. *Int J Mol Sci* 2020; **21** [PMID: 32138313 DOI: 10.3390/ijms21051723]

28 **Coradduzza D**, Cruciani S, Arru C, Garroni G, Pashchenko A, Jedea M, Zappavigna S, Caraglia M, Amler E, Carru C, Maioli M. Role of miRNA-145, 148, and 185 and Stem Cells in Prostate Cancer. *Int J Mol Sci* 2022; **23** [PMID: 35163550 DOI: 10.3390/ijms23031626]

29 **Li X**, Chen W, Li R, Chen X, Huang G, Lu C, Wen Z, Peng X, Liu K, Zhang C, Li H, Hu Y, Zhao Z, Tao L, Lai Y. Bladder cancer diagnosis with a four-miRNA panel in serum. *Future Oncol* 2022; **18**: 3311-3322 [PMID: 36047424 DOI: 10.2217/fon-2022-0448]

30 **Zhang JL**, Zheng HF, Li K, Zhu YP. miR-495-3p depresses cell proliferation and migration by downregulating HMGB1 in colorectal cancer. *World J Surg Oncol* 2022; **20**: 101 [PMID: 35354479 DOI: 10.1186/s12957-022-02500-w]

31 **Alves LF**, Geraldo MV. MiR-495-3p regulates cell migration and invasion in papillary thyroid carcinoma. *Front Oncol* 2023; **13**: 1039654 [PMID: 36776296 DOI: 10.3389/fonc.2023.1039654]

32 **Huang GM**, Zang HL, Geng YX, Li YH. LncRNA FAM83A-AS1 aggravates the malignant development of esophageal cancer by binding to miR-495-3p. *Eur Rev Med Pharmacol Sci* 2020; **24**: 9408-9415 [PMID: 33015782 DOI: 10.26355/eurrev_202009_23024]

33 **Yang H**, Guo J, Jin W, Chang C, Guo X, Xu C. A combined proteomic and metabolomic analyses of the priming phase during rat liver regeneration. *Arch Biochem Biophys* 2020; **693**: 108567 [PMID: 32898568 DOI: 10.1016/j.abb.2020.108567]

34 **Zhang C**, Chang C, Li D, Zhang F, Xu C. The novel protein C3orf43 accelerates hepatocyte proliferation. *Cell Mol Biol Lett* 2017; **22**: 21 [PMID: 28932249 DOI: 10.1186/s11658-017-0051-3]

35 **Li L**, Jiang D, Zhang Q, Liu H, Xu F, Guo C, Qin Z, Wang H, Feng J, Liu Y, Chen W, Zhang X, Bai L, Tian S, Tan S, Xu C, Song Q, Liu Y, Zhong Y, Chen T, Zhou P, Zhao JY, Hou Y, Ding C. Integrative proteogenomic characterization of early esophageal cancer. *Nat Commun* 2023; **14**: 1666 [PMID: 36966136 DOI: 10.1038/s41467-023-37440-w]

36 **Kwak AW**, Lee MJ, Lee MH, Yoon G, Cho SS, Chae JI, Shim JH. The 3-deoxysappanchalcone induces ROS-mediated apoptosis and cell cycle arrest *via* JNK/p38 MAPKs signaling pathway in human esophageal cancer cells. *Phytomedicine* 2021; **86**: 153564 [PMID: 33895649 DOI: 10.1016/j.phymed.2021.153564]

37 **Kim T**, Gartner A. Bub1 kinase in the regulation of mitosis. *Anim Cells Syst (Seoul)* 2021; **25**: 1-10 [PMID: 33717411 DOI: 10.1080/19768354.2021.1884599]

38 **Johnson VL**, Scott MI, Holt SV, Hussein D, Taylor SS. Bub1 is required for kinetochore localization of BubR1, Cenp-E, Cenp-F and Mad2, and chromosome congression. *J Cell Sci* 2004; **117**: 1577-1589 [PMID: 15020684 DOI: 10.1242/jcs.01006]

39 **Seeley TW**, Wang L, Zhen JY. Phosphorylation of human MAD1 by the BUB1 kinase in vitro. *Biochem Biophys Res Commun* 1999; **257**: 589-595 [PMID: 10198256 DOI: 10.1006/bbrc.1999.0514]

40 **Klebig C**, Korinth D, Meraldi P. Bub1 regulates chromosome segregation in a kinetochore-independent manner. *J Cell Biol* 2009; **185**: 841-858 [PMID: 19487456 DOI: 10.1083/jcb.200902128]

41 **Xu B**, Xu T, Liu H, Min Q, Wang S, Song Q. MiR-490-5p Suppresses Cell Proliferation and Invasion by Targeting BUB1 in Hepatocellular Carcinoma Cells. *Pharmacology* 2017; **100**: 269-282 [PMID: 28810242 DOI: 10.1159/000477667]

42 **Huang Z**, Wang S, Wei H, Chen H, Shen R, Lin R, Wang X, Lan W, Lin R, Lin J. Inhibition of BUB1 suppresses tumorigenesis of osteosarcoma *via* blocking of PI3K/Akt and ERK pathways. *J Cell Mol Med* 2021; **25**: 8442-8453 [PMID: 34337852 DOI: 10.1111/jcmm.16805]

43 **Yao LL**, Cao LY, Zhang HF, Li H, Yang F. Expression and clinical significance of Bub1 in esophageal squamous cancer. *Xiandai Zhongliu Yixue* 2011; **19**: 1726-1730

44 **Wei P**, He Q, Liu T, Zhang J, Shi K, Zhang J, Liu S. Baitouweng decoction alleviates dextran sulfate sodium-induced ulcerative colitis by suppressing leucine-related mTORC1 signaling and reducing oxidative stress. *J Ethnopharmacol* 2023; **304**: 116095 [PMID: 36581160 DOI: 10.1016/j.jep.2022.116095]

45 **Miao Z**, Chen L, Feng H, Gu M, Yan J, Xu Y, Ye B. Baitouweng Decoction Ameliorates Ulcerative Colitis in Mice Partially Attributed to Regulating Th17/Treg Balance and Restoring Intestinal Epithelial Barrier. *Front Pharmacol* 2020; **11**: 531117 [PMID: 33597862 DOI: 10.3389/fphar.2020.531117]

46 **Xuan-Qing CHEN**, Xiang-Yu LV, Shi-Jia LIU. Baitouweng decoction alleviates dextran sulfate sodium-induced ulcerative colitis by regulating intestinal microbiota and the IL-6/STAT3 signaling pathway. *J Ethnopharmacol* 2021; **265**: 113357 [PMID: 32891820 DOI: 10.1016/j.jep.2020.113357]

47 **Gu X**, Miao Z, Wang Y, Yang Y, Yang T, Xu Y. New Baitouweng decoction combined with fecal microbiota transplantation alleviates DSS-induced colitis in rats by regulating gut microbiota metabolic homeostasis and the STAT3/NF-κB signaling pathway. *BMC Complement Med Ther* 2022; **22**: 307 [PMID: 36424592 DOI: 10.1186/s12906-022-03766-z]

48 **Li D**, Yan M, Sun F, Song J, Hu X, Yu S, Tang L, Deng S. miR-498 inhibits autophagy and M2-like polarization of tumor-associated macrophages in esophageal cancer *via* MDM2/ATF3. *Epigenomics* 2021; **13**: 1013-1030 [PMID: 34114479 DOI: 10.2217/epi-2020-0341]

49 **Yang W**, Ma J, Zhou W, Zhou X, Cao B, Zhang H, Zhao Q, Fan D, Hong L. Molecular mechanisms and clinical implications of miRNAs in drug resistance of esophageal cancer. *Expert Rev Gastroenterol Hepatol* 2017; **11**: 1151-1163 [PMID: 28838272 DOI: 10.1080/17474124.2017.1372189]

50 **Xi Y**, Shen Y, Wu D, Zhang J, Lin C, Wang L, Yu C, Yu B, Shen W. CircBCAR3 accelerates esophageal cancer tumorigenesis and metastasis *via* sponging miR-27a-3p. *Mol Cancer* 2022; **21**: 145 [PMID: 35840974 DOI: 10.1186/s12943-022-01615-8]

51 **Jafarzadeh A**, Noori M, Sarrafzadeh S, Tamehri Zadeh SS, Nemati M, Chatrabnous N, Jafarzadeh S, Hamblin MR, Jafari Najaf Abadi MH, Mirzaei H. MicroRNA-383: A tumor suppressor miRNA in human cancer. *Front Cell Dev Biol* 2022; **10**: 955486 [PMID: 36313570 DOI: 10.3389/fcell.2022.955486]

52 **Wang LN**, Zhu XQ, Song XS, Xu Y. Long noncoding RNA lung cancer associated transcript 1 promotes proliferation and invasion of clear cell renal cell carcinoma cells by negatively regulating miR-495-3p. *J Cell Biochem* 2018; **119**: 7599-7609 [PMID: 29932248 DOI: 10.1002/jcb.27099]

53 **Eun JW**, Kim HS, Shen Q, Yang HD, Kim SY, Yoon JH, Park WS, Lee JY, Nam SW. MicroRNA-495-3p functions as a tumor suppressor by regulating multiple epigenetic modifiers in gastric carcinogenesis. *J Pathol* 2018; **244**: 107-119 [PMID: 28991363 DOI: 10.1002/path.4994]

54 **Liu P**, Shen JK, Hornicek FJ, Liu F, Duan Z. Wnt inhibitory factor 1 (WIF1) methylation and its association with clinical prognosis in patients with chondrosarcoma. *Sci Rep* 2017; **7**: 1580 [PMID: 28484252 DOI: 10.1038/s41598-017-01763-8]

55 **Piao XM**, You C, Byun YJ, Kang HW, Noh J, Lee J, Lee HY, Kim K, Kim WT, Yun SJ, Lee SC, Kang K, Kim YJ. Prognostic Value of BUB1 for Predicting Non-Muscle-Invasive Bladder Cancer Progression. *Int J Mol Sci* 2021; **22** [PMID: 34884561 DOI: 10.3390/ijms222312756]

56 **Jin J**, Xu H, Li W, Xu X, Liu H, Wei F. LINC00346 Acts as a Competing Endogenous RNA Regulating Development of Hepatocellular Carcinoma *via* Modulating CDK1/CCNB1 Axis. *Front Bioeng Biotechnol* 2020; **8**: 54 [PMID: 32133348 DOI: 10.3389/fbioe.2020.00054]

57 **Li M**, Shang H, Wang T, Yang SQ, Li L. Huanglian decoction suppresses the growth of hepatocellular carcinoma cells by reducing CCNB1 expression. *World J Gastroenterol* 2021; **27**: 939-958 [PMID: 33776365 DOI: 10.3748/wjg.v27.i10.939]

58 **Sunada S**, Saito H, Zhang D, Xu Z, Miki Y. CDK1 inhibitor controls G2/M phase transition and reverses DNA damage sensitivity. *Biochem Biophys Res Commun* 2021; **550**: 56-61 [PMID: 33684621 DOI: 10.1016/j.bbrc.2021.02.117]

59 **Huynh J**, Chand A, Gough D, Ernst M. Therapeutically exploiting STAT3 activity in cancer - using tissue repair as a road map. *Nat Rev Cancer* 2019; **19**: 82-96 [PMID: 30578415 DOI: 10.1038/s41568-018-0090-8]

60 **Liu H**, Ren G, Wang T, Chen Y, Gong C, Bai Y, Wang B, Qi H, Shen J, Zhu L, Qian C, Lai M, Shao J. Aberrantly expressed Fra-1 by IL-6/STAT3 transactivation promotes colorectal cancer aggressiveness through epithelial-mesenchymal transition. *Carcinogenesis* 2015; **36**: 459-468 [PMID: 25750173 DOI: 10.1093/carcin/bgv017]

61 **Hu X**, Ma J, Vikash V, Li J, Wu D, Liu Y, Zhang J, Dong W. Thymoquinone Augments Cisplatin-Induced Apoptosis on Esophageal Carcinoma Through Mitigating the Activation of JAK2/STAT3 Pathway. *Dig Dis Sci* 2018; **63**: 126-134 [PMID: 29197940 DOI: 10.1007/s10620-017-4856-8]

62 **Liu Y**, Wang X, Zeng S, Zhang X, Zhao J, Zhang X, Chen X, Yang W, Yang Y, Dong Z, Zhu J, Xu X, Tian F. The natural polyphenol curcumin induces apoptosis by suppressing STAT3 signaling in esophageal squamous cell carcinoma. *J Exp Clin Cancer Res* 2018; **37**: 303 [PMID: 30518397 DOI: 10.1186/s13046-018-0959-0]

63 **Wu L**, Qian C, Zhang W, Shi M, Chen X, Wang Y, Lin F. Ginkgetin suppresses ovarian cancer growth through inhibition of JAK2/STAT3 and MAPKs signaling pathways. *Phytomedicine* 2023; **116**: 154846 [PMID: 37172479 DOI: 10.1016/j.phymed.2023.154846]

64 **Resetca D**, Haftchenary S, Gunning PT, Wilson DJ. Changes in signal transducer and activator of transcription 3 (STAT3) dynamics induced by complexation with pharmacological inhibitors of Src homology 2 (SH2) domain dimerization. *J Biol Chem* 2014; **289**: 32538-32547 [PMID: 25288792 DOI: 10.1074/jbc.M114.595454]

65 **Robker RL**, Watson LN, Robertson SA, Dunning KR, McLaughlin EA, Russell DL. Identification of sites of STAT3 action in the female reproductive tract through conditional gene deletion. *PLoS One* 2014; **9**: e101182 [PMID: 24983622 DOI: 10.1371/journal.pone.0101182]

66 **Don-Doncow N**, Escobar Z, Johansson M, Kjellström S, Garcia V, Munoz E, Sterner O, Bjartell A, Hellsten R. Galiellalactone is a direct inhibitor of the transcription factor STAT3 in prostate cancer cells. *J Biol Chem* 2014; **289**: 15969-15978 [PMID: 24755219 DOI: 10.1074/jbc.M114.564252]

67 **Zhu S**, Phatarpekar PV, Denman CJ, Senyukov VV, Somanchi SS, Nguyen-Jackson HT, Mace EM, Freeman AF, Watowich SS, Orange JS, Holland SM, Lee DA. Transcription of the activating receptor NKG2D in natural killer cells is regulated by STAT3 tyrosine phosphorylation. *Blood* 2014; **124**: 403-411 [PMID: 24891320 DOI: 10.1182/blood-2013-05-499707]

Published by **Baishideng Publishing Group Inc**
7041 Koll Center Parkway, Suite 160, Pleasanton, CA 94566, USA
Telephone: +1-925-3991568
E-mail: office@baishideng.com
Help Desk: https://www.f6publishing.com/helpdesk
https://www.wjgnet.com